

DESIGN, FABRICATION AND TESTING OF A MICROMACHINED SEISMOMETER WITH NANO-G RESOLUTION

W.T. Pike¹, I. M. Standley², W.J. Karl¹, S. Kumar¹, T. Semple¹, S. J. Vijendran¹ and T. Hopf¹

¹Electrical and Electronic Engineering, Imperial College London, UK

²Kinematics Inc, Pasadena, California, USA

ABSTRACT

We have designed a high resolution microseismometer by combining a low-resonant-frequency, high-quality-factor suspension with a sensitive lateral capacitive transducer under electromagnetic feedback control. It has been fabricated and tested to demonstrate for the first time a micromachined seismometer capable of resolving the Earth's ambient seismicity and with the best acceleration resolution of any micromachined device to date, with a self noise down to $4 \text{ ng}/\sqrt{\text{Hz}}$.

KEYWORDS

Micromachining; seismometer; accelerometer; noise

INTRODUCTION

Although micromachined accelerometers are now dominant in the measurement of shocks and vibrations at higher levels [1], there are considerable challenges in extending the resolution down to the seismic noise of the Earth, a range of considerable interest for geophysical investigation and exploration. A major challenge to miniaturizing high resolution accelerometers is that the inherent acceleration noise spectral density for any lossy suspension increases as the mass and the resonant period are reduced [2]. Hence reducing the size of a device will in general push up its noise floor, although this can be compensated if the quality factor, Q , of the suspension can be increased. Such an increase can be achieved firstly by using low loss materials, such as single-crystal silicon, to form the suspension and secondly by reducing gas damping either through geometry or by reducing the gas pressure into the rarefied regime.

A further challenge is to incorporate a sensitive enough transducer to reduce the inevitable contribution of

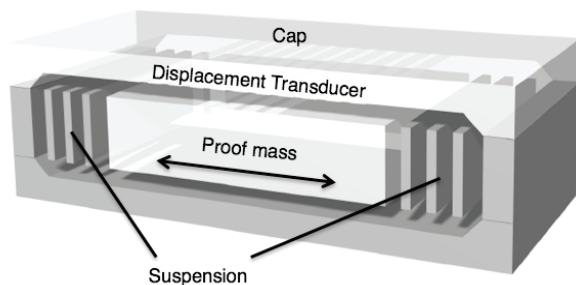


Figure 1.: Schematic view of the microseismometer in cross section

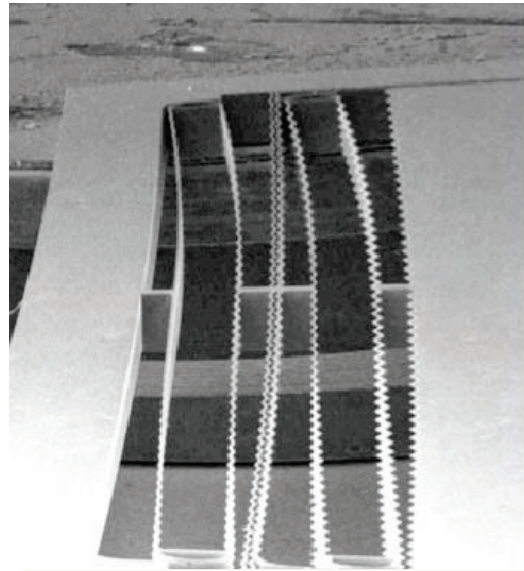


Figure 2: Micrograph of one half of the suspension of the microseismometer. The die is $20 \text{ mm} \times 20 \text{ mm}$. The dynamics of the suspension are evident as a beating between the vibration of the device and a raster of the scan of the scanning electron microscope [3].

the electronics noise to the overall noise floor. Capacitance transducers have the necessary performance, but can themselves contribute to the gas damping due to the small electrode spacing necessary to provide a large displacement signal. Rather than rely on evacuation, the design presented here minimizes gas damping through the geometry of the displacement transducer, while using the maximum proof mass and lowest resonant frequency that the device size allows.

DESIGN

Figure 1 shows a schematic cross-section through the device. A wafer is micromachined to produce the proof mass and suspension in a single-crystal silicon die which is sandwiched between two capping dies. The suspension is lateral and in the plane of the silicon die with individual flexures of width $30 \mu\text{m}$ and thickness $525 \mu\text{m}$ (figure 2). The self noise is minimized by using as large a proof mass as possible, combined with comparatively weak springs to reduce the resonant frequency. Through-wafer deep reactive-ion etching (DRIE) of a 20 mm die gives the

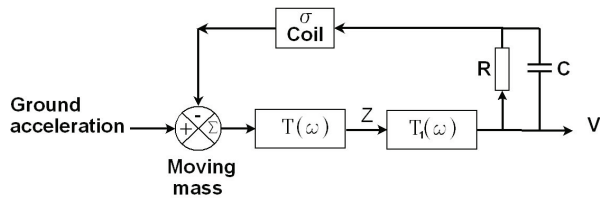


Figure 3. Control loop of the microseismometer. T and T_1 are the transfer function of the suspension and displacement transducer respectively. Z is the displacement and V is the output.

proof mass the full thickness of the wafer, with a resonant frequency of around 10 Hz. Intermediate frames ensure that the out-of-plane motion is minimized as well as increasing the frequency of all spurious off-axis modes [4]. This gives a clean response to above 100 Hz.

The electrodes of the displacement transducer are patterned on the top of the proof mass and the inner surface of the cap of figure 2. The electrodes are arrayed laterally to produce a periodic output with displacement as the fixed and moving electrodes move in and out of synchronicity. This ensures that the small electrode gap necessary for large capacitance gain results in Couette rather than the much larger squeeze-film damping as the dominant contribution from gas flow within the capacitance transducer. To further reduce this damping the cap is relieved to increase the channel available for gas flow away from the electrodes.

The device is designed to be operated in feedback (figure 3). The periodic output of the transducer provides a number of possible operating points for the feedback. Hence if the background signal is large, as is the case for a vertical-axis seismometer which has to measure the seismic signal against the gravitational force of the earth, the suspension can move to the closest null point for operation, minimizing the actuation force required to close the loop. The transducer output signal is then used to produce this feedback force using an electromagnetic actuator. The actuator consists of a series of coils on the proof mass and an external magnetic circuit which together provide a Lorentz force to drive the proof mass to the nearest control point of the displacement transducer. The large proof mass precludes the use of weaker electrostatic actuation.

FABRICATION

The proof mass and suspension of the microseismometer are fabricated from a single-crystal silicon wafer. An oxide layer insulates the silicon substrate from the electrodes and the coils formed on one surface of the wafer. A metal1-dielectric-metal2 multilayer structure is used to provide the topology required for multiple-turn coils as well as guard electrodes between the capacitance transducer electrodes and the substrate (figure 4). This

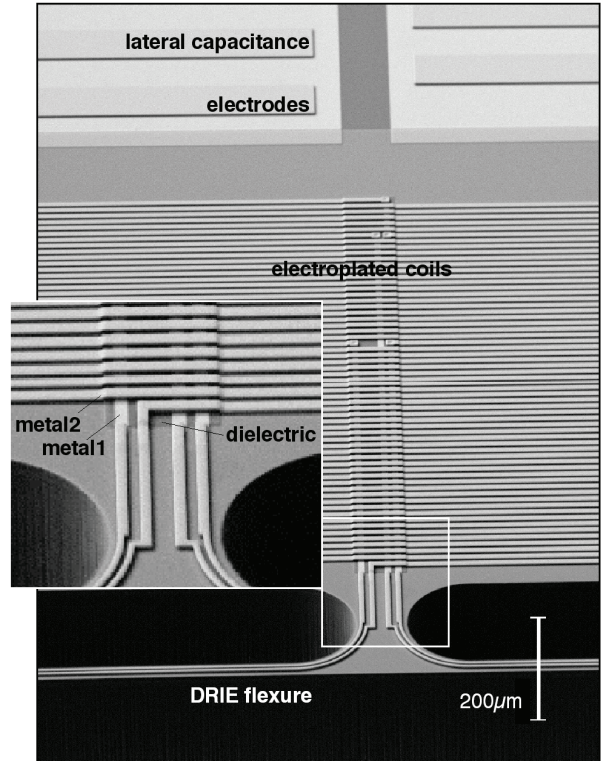


Figure 4.: Micrograph of the microseismometer structure showing the processed layers.

multilayer structure is fabricated by patterning first a sputtered metal, then a dielectric and finally an electrodeposited metal layer. Electrodeposition ensures that the coils have sufficient cross-sectional area to carry the levitating currents required to hold the proof mass at one of the operating points. Connections to the transducer electrodes and coils on the proof mass are made with electrodeposited traces routed as pairs along each spring. The through-wafer DRIE subsequently forms the suspension as well as singulating the dies. The DRIE used

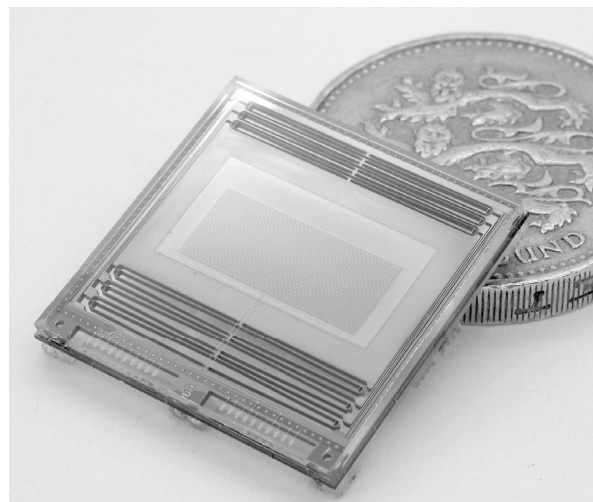


Figure 5: The packaged microseismometer

a halo mask with an etch width of 40 μm to optimize the side-wall geometry of the flexures [5].

The glass capping dies which carry the fixed electrodes of the displacement transducer are fabricated by patterning of sputtered metal followed by abrasive cutting that provides both the relief for gas flow and singulates the dies. Solder bonding of the silicon and capping dies routes all the electrical connections on to the glass die. The bonds are formed by reflow of 100- μm solder balls on metal pads and ensure lateral alignment as well as the controlled spacing of the dies which sets the gap between the electrodes of the transducer. Finally, a glass backing die, with abrasively cut cavities, is mounted on the back of the silicon die to provide protection while providing a further path for gas flow around the proof mass. Fig. 5 shows the completed microseismometer die.

ELECTRONICS

This die is mounted in a magnetic circuit to provide the feedback actuator and connected to the external electronics. These electronics first measure the capacitance change due to the motion of the proof mass by demodulating the differential output from the fixed cap electrodes due to opposed sinusoidal drive signals on the proof-mass electrodes. This displacement signal is the input to the feedback electronics which provide the current actuation signals to the coils. The feedback is separately applied to an integral coil which centers the proof mass at the closest operating point of the displacement transducer and a main coil which operates in the seismic bandwidth of the device and provides a velocity output signal.

TEST RESULTS

Seismic testing was carried out alongside a conventional high performance seismometer in a seismic vault. Fig. 6 shows a remote seismic event, a magnitude 7 earthquake near the Sandwich Islands recorded at Pasadena, CA by both the micromachined and conventional seismometers. Differences between the two traces are mainly due to misalignment between the axes of the two seismometers and the extension of the transfer function of the microseismometer to higher frequencies compared to the conventional instrument. The arrival of the various phases of the teleseismic event is nevertheless in good agreement between the two traces.

To measure the noise floor of the microseismometer, extended testing was conducted with both instruments. The ambient noise of the microseismometer is shown in figure 7 for frequencies below 1 Hz. Down to 0.1 Hz the signal is dominated by an ambient microseismic peak due to oceanic coupling to the lithosphere.

Below the 0.1 Hz the ambient seismicity drops off sharply, as confirmed by the conventional seismometer, and the self noise of the microseismometer becomes evident at a value between 3 and 4 $\text{ng}/\sqrt{(\text{Hz})}$ down to 0.04

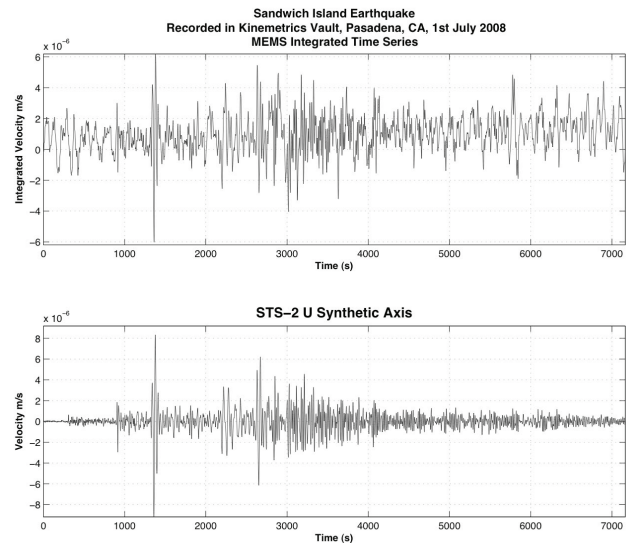


Figure 6.: Comparison between the seismic signal from the microseismometer (top) and a conventional seismometer from a magnitude 7 teleseismic event at an angular distance of 120° . The top trace has not been corrected for the transfer function of the microseismometer

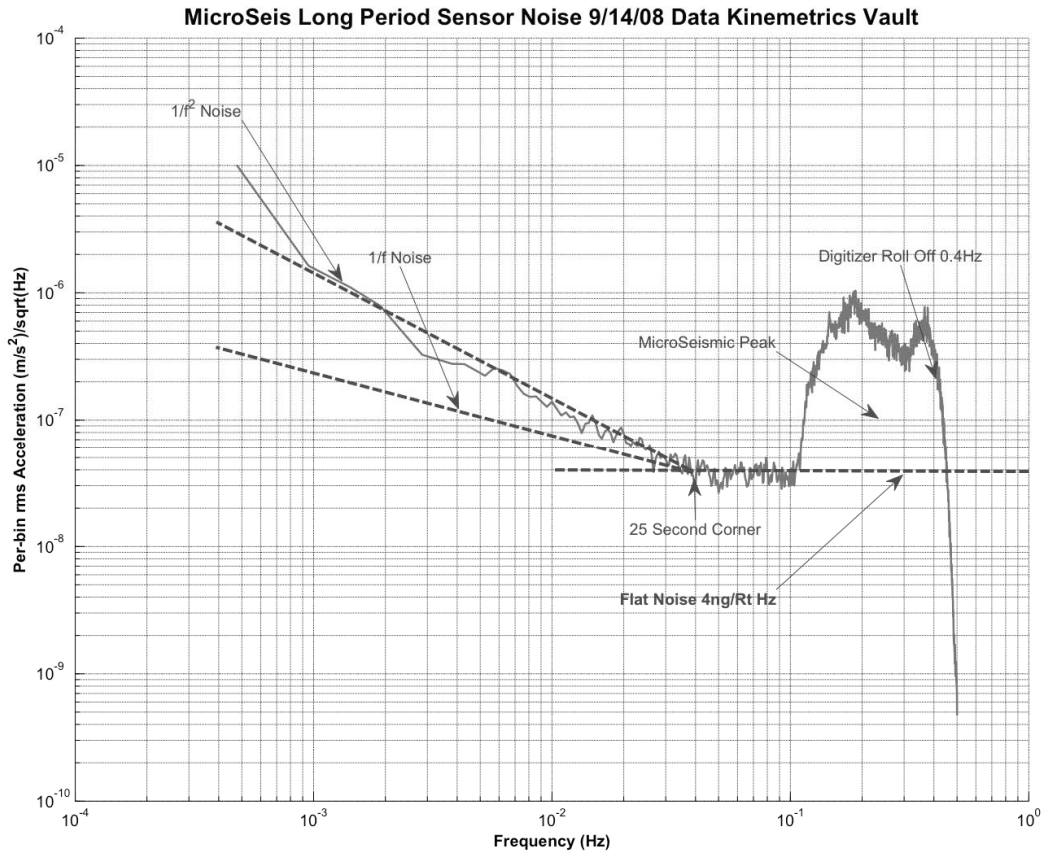
Hz. For this device the theoretical suspension noise derived from measured values of the resonant frequency, Q factor and proof mass is about $1 \text{ ng}/\sqrt{(\text{Hz})}$. Hence the microseismometer is within a factor of four of its absolute limit.

Below these frequencies the noise rises inversely as the square of frequency, consistent with drift in the microseismometer signal, rather than with electronics noise which should rise more shallowly as the reciprocal of frequency. A correlation with temperature measurements at these frequencies indicates that thermal drift is the most likely cause of this noise.

CONCLUSIONS

We have designed fabricated and tested a microseismometer with an unprecedented resolution below $4 \text{ ng}/\sqrt{(\text{Hz})}$. The barriers to this level of performance in a micromachined device were overcome by using through-wafer etching to maximize the proof mass, weak flexures fabricated in single-crystal silicon to keep the resonant frequency low and material quality factor high, and a suspension, transduction and packaging geometry to keep the gas damping low. Furthermore the lateral capacitance array transducer used in this microseismometer had sufficient gain to ensure that the electronics noise did not dominate the performance.

The self noise of the device is shown to be close to its theoretical limits up to periods of 25 s. Further reduction of the gas damping by increased relief of the capping die



should reduce the theoretical limits and indicate the contribution of the electronic noise to the performance. At periods greater than 25 s the drift of the device is apparent, with the thermal response of the device likely dominating.

ACKNOWLEDGEMENTS

We would like to thank the UK Science and Technology Facilities Council and the Air Force Research Laboratory for financial support and Irek Briones at Kinematics for assistance with the testing.

REFERENCES

- [1] N. Yazdi, F. Ayazi, and K. Najafi, "Micromachined inertial sensors," *Proc. IEEE*, vol. 86, pp. 1640–1659, 1998.
- [2] T. B. Gabrielson, "Mechanical–thermal noise in micromachined acoustic and vibration sensors" *IEEE Trans Electron Dev* 40 pp. 903–909, 1993.
- [3] W. T. Pike and I.M. Standley, "Determination of the dynamics of micromachined lateral suspensions in the scanning electron microscope" *J Micromech Microengineering*, Vol. 15 pp S82-S88, 2005.
- [4] W. T. Pike and S. Kumar, "Improved design of micromachined lateral suspensions using intermediate frames," *J. Micromech. MicroEng.* Vol. 17 pp 1680-

1694, 2007.

- [5] W. T. Pike, W. J. Karl, S. Kumar, S. Vijendran, and T. Semple, T. "Analysis of sidewall quality in through-wafer deep reactive-ion etching" *Microelectron.Eng.*, Vol. 73-74, pp 340-345, 2004.

CONTACT

* W. T. Pike, tel: +44 20 7594 6207;
w.t.pike@imperial.ac.uk